Theor Chem Acc (2010) 126:27–37
DOI 10.1007/s00214-009-0668-z

REGULAR ARTICLE

Theoretical study in gas phase of linear and nonlinear optical properties of the *ortho*-, *meta*- and *para*-nitrophenol isomers

Johan Urdaneta · Yaneth Bermúdez · Federico Arrieta · Merlin Rosales · Néstor Cubillán · Javier Hernández · Olga Castellano · Humberto Soscún

Received: 20 May 2009 / Accepted: 19 October 2009 / Published online: 18 November 2009

Abstract The linear (α), and nonlinear (β, γ) optical NLO properties of *ortho*-, *meta*- and *para*-nitrophenol (ONP, MNP and PNP) isomers have been calculated in gas phase by using ab initio (HF, MP2 and MP4) and density functional theory (DFT) (B3LYP, CAM-B3LYP) methods, with the 6-31+G(d,p) and 6-311+G(3d,3p) standard and the Sadlej specialized basis sets. These properties were evaluated both at static and at dynamic regime within the finite field FF numerical techniques and the time-dependent-Hartree–Fock approach at 1,910 nm, respectively. Additional calculations were performed for the β static hyperpolarizability of these isomers in presence of *p*-dioxane solvent with the Onsager Model and the SCRF-PCM approach, using B3LYP/6-31+G(d,p) and MP2/6-31+G(d,p) levels of theory. Additionally, CCSD/6-31+G(d,p) calculations were performed for the α, β and γ properties of PNP isomer. The B3LYP and MP2 α_{ave} results of the nitrophenol isomers are comparable to the experimental α_{ave} reports; while the tendency for the β_v calculated values (β_v PNP $>$ β_v MNP $>$ β_v ONP), that can be explained in terms of the O_x atomic charge of the $-NO_2$ group, does not follow exactly the experimental ones. The B3LYP γ_{ave} results are in correspondence to the experimental measurements, the correlation of which is $r^2 = 0.99$. The use of FF methodology in conjunction with the B3LYP and MP2 methods and the 6-31+G(d,p) basis set show to be appropriate approaches to predict qualitative optical properties of Push–Pull like organic molecules, provided are considered the solvent effects or frequency dependence. However, to have a clear picture of the NLO properties of an isolated molecule, higher order correlation effects combined with specialized basis sets, frequency and solvent effects should be employed. We have demonstrated that MP4/Sadlej level of theory is able to reproduce NLO properties that can be considered equivalent to those from more sophisticated approaches, such as CCSD together with extended basis sets.

Keywords Push–Pull molecules · Finite field approach · Optical properties · Nitrophenol isomer · *Para*-nitroaniline

Electronic supplementary material The online version of this article (doi:10.1007/s00214-009-0668-z) contains supplementary material, which is available to authorized users.

J. Urdaneta · Y. Bermúdez · F. Arrieta · H. Soscún
Laboratorio de Química Inorgánica Teórica,
Departamento de Química, Facultad Experimental de Ciencias,
Universidad del Zulia, Apdo. 526, Maracaibo, Venezuela
e-mail: johansub@gmail.com

M. Rosales
Laboratorio de Química Inorgánica, Departamento de Química,
Facultad Experimental de Ciencias, Universidad del Zulia,
Apdo. 526, Maracaibo, Venezuela

N. Cubillán
Laboratorio de Electrónica Molecular,
Departamento de Química, Facultad Experimental de Ciencias,
Universidad del Zulia, Apdo. 526, Maracaibo, Venezuela

J. Hernández · O. Castellano
Departamento de Procesamiento de Residuales y Crudos
Pesados, Urbanización Santa Rosa, PDVSA-INTEVEP,
Sector El Tambor, Los Teques, Edo. Miranda,
Apdo. 76343, Caracas 1070-A, Venezuela

H. Soscún (✉)
Centro Nacional de Tecnología Química CNTQ,
Complejo Tecnológico Simón Rodríguez CTSR,
La Carlota, Caracas, Venezuela
e-mail: hsoscun@gmail.com; hsoscun@yahoo.es

1 Introduction

The study of the linear and nonlinear (NLO) optic properties plays a key role in the understanding of the electronic behavior of molecular structures in presence of external electric fields. This knowledge facilitates the design of new materials with technological applications in the area of telecommunications, electro-optics and computer engineering [1].

Experimentally, the NLO properties of materials are its responses to the electric field perturbations exposed as different optical phenomena, which are characterized by particular combination of frequencies (ω) [2–4]. At theoretical level, these properties can be determined by quantum mechanic procedures, through either the derivatives of the energy or dipole moment with respect to the applied field [2, 5–7]. However, the accuracy in the calculations of the optical properties in comparison to the experimental measurements depend on several factors which are mainly due to the selection of the quantum method and basis sets, and also to the frequency of the applied electric field, the solvent effect polarity and the nuclear vibrational contribution, among others. A great variety of reports have been published addressing the different approximations in terms of Hamiltonians and basis sets that can be able to reproduce the existent experimental data of electric properties of molecules in gas phase and in solution [6]. It is important to mention the very recent work of Hammond and Kowalski [7], that treat the parallel computations of static hyperpolarizabilities of single molecules in gas phase (water, acetonitrile, chloroform and *para*-nitroaniline) with a large selection of basis sets using coupled-cluster (CC) response theory and four density functional theory methods. The impact of these results will be considered in Sect. 2.

On the other hand, the most of the theoretical studies related to nonlinear optical properties are oriented to the characterization of organic compounds, mainly based on structures that have electron donor (D) and electron acceptor (A) groups linked to the extremes of a conjugated π bond network. This kind of system, referred as Push–Pull, is a model that is useful to explain the NLO behavior of excellent molecular candidates [3, 4, 8]. A typical example of this model is the *p*-nitroaniline (PNA) compound, which is considered a standard in various experimental and theoretical optical processes due to its high NLO responses [9–12]. The aim of the present work is to evaluate the effect of the substitution of the NH_2 by the -OH group on the NLO properties in PNA, leading to the *p*-nitrophenol (PNP) compound. Additionally, we study the effect of changing the position of the hydroxyl group into the benzene ring to give the *o*-nitrophenol (ONP) and *m*-nitrophenol (MNP) isomers. Few experimental and theoretical reports have been published so far for the linear and nonlinear optical properties of nitrophenol isomers. In particular, Cheng et al. [13–15] reported EFISH and THG measurements at 1,910 nm in dioxane of nitrophenol compounds. Bursy et al. [16] reported the static and dynamic ($\omega = 1{,}064$ nm) optical properties of these molecules using the sum over orbitals (SOO) method at level of HF with different basis sets. Finally, Guthmuller and Simon [17] determined the static and dynamic ($\omega = 1{,}910$ nm) first hyperpolarizability β of PNP at DFT level using the SAOP functional and the TZ2P basis set.

In this work, we explore the performance of the available quantum chemistry methods and basis sets, including dynamic and solvent effects, on the dipole (hyper)polarizabilities of these isomers and the possibility that they could represent a good alternative of building blocks for the synthesis of new NLO materials based on this system. Calculations for *p*-nitroaniline molecule PNA were also performed for comparison and record purposes. The present theoretical study has been also oriented to evaluate the electronic contribution in gas phase to the linear and nonlinear optical properties, at static ($\omega = 0$ nm) and dynamic ($\omega = 1{,}910$ nm) regime, of the *o*-, *m*- and *p*-nitrophenol molecules, using the finite field (FF) methodology at the ab initio and DFT levels, using a series of extended basis sets augmented with single and multiple *d* and *p* polarization and *s* and *sp* diffuse functions. Additional calculations were performed by using the high-level coupled-cluster (CC) approach. A comparison between the present theoretical results and the experimental and theoretical existent data is made for the studied molecules.

2 Theory and computational details

When an electric field $\vec{F}$ interacts with a material a displacement of charges induces a bulk polarization. At microscopic level, the molecular polarization can be expressed in terms of the induced dipole moment μ_i through a Taylor expansion series in terms of the applied field components [5–7]:

$$\mu_i(\vec{F}) = \mu_0 + \sum_j \alpha_{ij} \cdot \vec{F}_j + \left(\frac{1}{2}\right) \sum_{jk} \beta_{ijk} \cdot \vec{F}_j \cdot \vec{F}_k + \left(\frac{1}{6}\right) \sum_{jkl} \gamma_{ijkl} \cdot \vec{F}_j \cdot \vec{F}_k \cdot \vec{F}_j \ldots \quad (1)$$

where, $\mu_i(\vec{F})$ is the permanent dipole moment, α_{ij} is the linear dipole polarizability, while β_{ijk} and γ_{ijkl} are the first and second hyperpolarizability, respectively, that correspond to the macroscopic nonlinear optical properties. The subscripts *i, j, k* and *l* represent the coordinates of reference for the molecular system.

The Eq. 1 can be also represented as the energy of the system E in function of the electric field as shown in the following equation,

$$E\left(\vec{F}\right) = \vec{E}_0 - \sum_i \mu_i \vec{F} - \left(\frac{1}{2}\right)\sum_{ij} \alpha_{ij} \cdot \vec{F}_i \cdot \vec{F}_j - \left(\frac{1}{6}\right)\sum_{ijk} \beta_{ijk} \cdot \vec{F}_i \cdot \vec{F}_j \cdot \vec{F}_k - \left(\frac{1}{24}\right)\sum_{ijkl} \gamma_{ijkl} \cdot \vec{F}_i \cdot \vec{F}_j \cdot \vec{F}_k \cdot \vec{F}_{j\ldots} \quad (2)$$

where, $\vec{E}_0$ is the energy of the molecule in absence of the field and the coefficients of both equations are defined as:

$$\mu_i = -\left(\frac{\partial E(F)}{\partial F_i}\right)_{F\to w} \quad (2a)$$

$$\alpha_{ij} = -\left(\frac{\partial^2 E(F)}{\partial F_i \partial F_j}\right)_{F\to w} \quad (2b)$$

$$\beta_{ijk} = -\left(\frac{\partial^3 E(F)}{\partial F_i \partial F_j \partial F_k}\right)_{F\to w} \quad (2c)$$

$$\gamma_{ijkl} = -\left(\frac{\partial^4 E(F)}{\partial F_i \partial F_j \partial F_k \partial F_l}\right)_{F\to w} \quad (2d)$$

The quantities of experimental interest that are related to the linear and nonlinear optical molecular properties, which represent averages and invariant with respect to the coordinate system, are given by the following equations.

$$\alpha_{\text{ave}} = \frac{1}{3}\left(\alpha_{xx} + \alpha_{yy} + \alpha_{zz}\right) \quad (3)$$

$$\beta_v = \frac{1}{3}\left(\beta_{iii} + \beta_{ijj} + \beta_{ikk}\right) \quad (4)$$

$$\gamma_{\text{ave}} = \frac{1}{5}\left[\gamma_{xxxx} + \gamma_{yyyy} + \gamma_{zzzz} + 2\left(\gamma_{xxyy} + \gamma_{xxzz} + \gamma_{yyzz}\right)\right] \quad (5)$$

where, α_{ave} is the average polarizability, β_v is the main component of the first hyperpolarizability β tensor calculated with respect to the direction of the dipole moment [6] and γ_{ave} is the average of the second hyperpolarizability tensors.

In this work, the static optical (α, β and γ) properties of the nitrophenol isomers were calculated using ab initio HF, MP2 and MP4 methods and the density functional theory B3LYP and CAM-B3LYP hybrid approaches, in conjunction with the standard 6-31+G(d,p), 6-311++G(3d,3p) and the specialized Sadlej basis sets [18–30]. These methodologies, with the exception of the CAM-B3LYP, were applied within the context of finite field FF methodology [31], employing the equations of Kurtz [32] th intensity of the electric field components of which is of 0.005 au. The Kurtz equations were codified in the fortran 77 FFIELD software, designed and developed at the Laboratory of Theoretical and Inorganic Chemistry of La Universidad del Zulia, as an interface for the Gaussian 98 and Gaussian 03 [33] computational programs to allow the evaluation of energies at different electric field components at Hartre-Fock and post-Hartree–Fock theory levels, and internal and external basis sets, to calculate the energy numeric derivatives and obtaining the components of the microscopic linear and nonlinear optical property tensors of the considered molecules. This procedure is able to calculate the NLO properties in gas phase and in solution. In particular, the CAM-B3LYP DFT calculations were carried out with the Dalton program [34].

The calculations of the dynamic optical properties were performed within the time-dependent Hartree–Fock (TDHF) approach and the 6-31+G(d,p) basis set, available in the GAMESS [35] computational program. In this case, the derivatives are evaluated by analytic methods and the static and dynamic (hyper)polarizability components are calculated independently at Hartree–Fock level [36]. An estimate of the optical properties at TD-MP2 and TD-B3LYP levels were obtained through the following relationship [37]:

$$x^n_{\text{correlation}}(\text{dynamic}) = \left[\frac{x^n_{\text{correlation}}(\text{static})}{x^n_{\text{SCF}}(\text{static})}\right] \cdot x^n_{\text{SCF}}(\text{dynamic}) \quad (6)$$

Additionally, we have also made calculations for the β static hyperpolarizability of the nitrophenol isomers in presence of *p*-dioxane solvent using both, the Onsager Model and the SCRF-PCM approach [38–41] at B3LYP/6-31+G(d,p) and MP2/6-31+G(d,p) levels of theory, within the FF scheme with the Gaussian software. All the calculations, gas phase and solution, were performed using fully optimized geometric structures, and restricted symmetry (*Cs*) at the different levels of theory, whereas the PNA molecule was restricted to C_2v symmetry. Finally, CCSD/6-31+G(d,p) calculations [18–30] were performed within the FF methodology and the Gaussian software for the PNP isomer.

3 Results and discussion

A representation of the studied molecules with the orientation of the coordinate system is displayed in Fig. 1. It is important to note that the optimized geometric parameters of these molecules obtained in this work agree reasonably with its experimental results of X-ray diffraction [42–46].

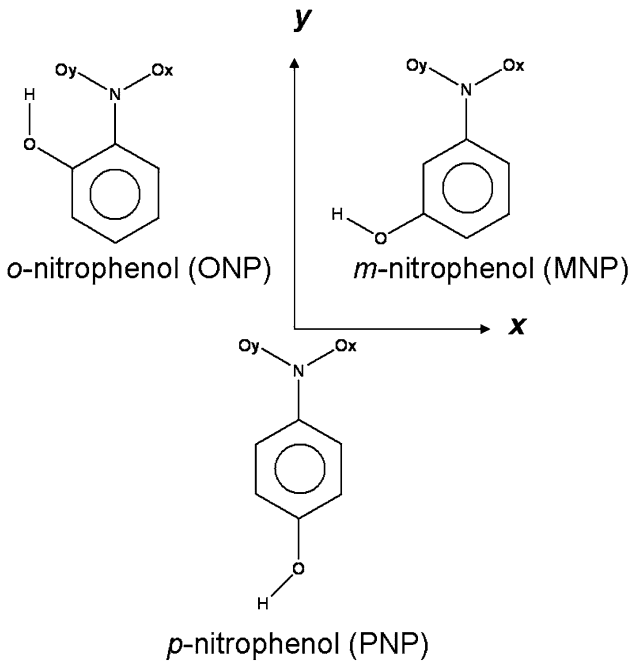

Fig. 1 Schematic representation and orientation axis for the ONP, MNP and PNP isomers. Similar orientation is used for the PNA molecule

3.1 Dipole moment (μ)

In this work, the μ, α, β and γ electronic properties of nitrophenol isomers, shown in Fig. 1, were calculated at the HF, MP2, MP4, B3LYP and CAM-B3LYP levels of theory, using the A = 6-31+G(d, p), B = 6-311++G(3d,3p) and the C = Sadlej basis sets and fully *Cs* optimized geometries. The HF and B3LYP results, not only for the dipole moments but also for the rest of the calculated properties are included as supplementary material. The calculated dipole moments μ and the corresponding experimental ones for each molecule are shown in Table 1, where a reasonable agreement exists between them. In fact, there are not significant differences between the μ values obtained with the variety of methods and the employed basis sets. However, the best theory–experiment concordance for the gas phase nitrophenol μ results is determined by the MP4/Sadlej methodology, as expected. The DFT calculations at the B3LYP and CAMB3LYP overestimate the experimental dipole moments of the nitrophenol isomers, including that of PNA, whereas the CCSD/A method is able to give a very good value for the μ for PNP molecule (4.90 Debyes), which reproduce within the experimental error the experimental dipole moment (5.0 Debyes) [13]. There are two important features in these values of Table 1: (i) The substitution of the NH_2 group in PNA by the OH to give the nitrophenol compounds that increase the dipole moment μ, where the maximum dipole moment is found for the *p*-nitrophenol isomer; (ii) The *o*- and *m*-isomers present similar values in the calculated dipole moment.

3.2 Linear polarizability (α)

The results for the α_{ii} components and the average dipole polarizability α_{ave} of ONP, MNP and PNP isomers, together with experimental [13] and theoretical [16] reports from the literature, are shown in Table 2. The corresponding results for the HF and B3LYP are included as supplementary material. The experimental α_{ave} of these isomers have been measured in *p*-dioxane and the corresponding static values were reported, indicating that MNP is the molecule with the lowest dipole polarizability of the isomer series, whereas the ONP and PNP species have almost the same α_{ave} value [13–15]. In addition, reports for nitrophenol α_{ave} calculations at the SOO-HF/TZVP level of theory indicate that the isomers posses almost the same dipole polarizability value, which are both smaller than the experimental ones and also they do not follow exactly the experimental trend. In the present work, a systematic study of this property has been performed in order to clarify the right order of the substituted nitrophenol polarizability.

Table 1 Calculated and experimental dipole moments μ(Debyes) of the ONP, MNP and PNP isomers

Molecule	μ (Debyes)										
	CAM-B3LYP			MP2			MP4			CCSD	Exp
	A	B	C	A	B	C	A	B	C	A	
ONP	4.05	3.87	3.95	3.52	3.35	3.32	3.59	3.42	3.40		3.4[a]
MNP	3.75	3.71	3.70	3.28	3.29	3.30	3.34	3.34	3.35		3.6[a]
PNP	5.48	5.36	5.41	4.87	4.78	4.79	4.93	4.84	4.85	4.90	5.0[a]
PNA	7.48	7.37	7.17	7.00	6.84	6.82	7.02	6.87	6.88		6.2[b]

Values for PNA are included for comparison. The basis sets are: A = 6-31+G(d.p); B = 6-311++G(3d.3p); C = Sadlej

[a] Experimental values in *p*-dioxane, Ref. [13]

[b] Experimental values in acetone, Ref. [13]

Table 2 Theoretical components α_{ii} and average dipole polarizabilitiy α_{ave} (au) at static regime of the ONP, MNP and PNP isomers

Molecule	α_{ave} (au)	CAM-B3LYP			MP2			MP4			Other studies
		A	B	C	A	B	C	A	B	C	
ONP	α_{xx}	106.33	109.22	109.99	106.41	109.84	110.57	104.48	107.87	108.71	
	α_{yy}	119.30	124.35	125.43	119.63	125.95	126.68	113.25	119.29	120.16	
	α_{zz}	47.10	51.22	51.40	47.31	52.27	53.05	46.69	51.58	52.36	
	α_{ave}	90.91	94.93	95.61	91.12	96.02	96.76	88.14	92.91	93.74	79.41[a] 101.22[b]
MNP	α_{xx}	104.48	108.40	108.27	105.48	109.16	109.85	104.36	107.95	108.72	
	α_{yy}	114.61	120.76	120.18	113.19	119.71	120.48	108.25	114.35	115.30	
	α_{zz}	46.89	51.27	51.56	47.12	52.22	53.14	46.44	51.48	52.40	
	α_{ave}	88.66	93.48	93.34	88.60	93.69	94.49	86.35	91.26	92.14	78.81[a] 87.73[b]
PNP	α_{xx}	100.14	103.13	104.11	98.38	101.79	102.37	96.76	100.74	100.74 (97.59)[d]	
	α_{yy}	124.53	129.78	131.88	126.18	133.16	134.14	120.30	126.951	128.14 (119.72)[d]	
	α_{zz}	46.79	51.23	51.66	47.02	52.15	53.07	46.37	51.434	52.36 (46.00)[d]	
	α_{ave}	90.48	94.71	95.89	90.53	95.70	96.53	87.81	92.820	93.75 (87.77)[d]	78.78[a] 101.22[b]
PNA	α_{xx}	96.10	99.20	100.06	101.01	105.02	105.81	98.98	102.92	103.76	
	α_{yy}	142.98	148.93	150.09	148.35	156.26	158.01	140.31	147.92	149.80	
	α_{zz}	49.68	53.92	54.37	50.96	56.09	57.16	50.16	55.20	56.26	
	α_{ave}	96.25	100.68	101.51	100.11	105.79 (120.18)[e] (124.07)[f] (120.28)[g]	106.99	96.49	102.02	103.27	114.73[c]

Values for PNA molecule are included for comparison. The basis sets are: A = 6-31+G(d.p); B = 6-311++G(3d.3p); C = Sadlej

[a] SOOHF/TZVP calculations; Ref. [16]

[b] Static experimental values in *p*-dioxane; Ref. [13]

[c] Static experimental value in acetone; Ref. [13]

[d] CCSD/C calculations (this work)

[e] Onsager (B3LYP/A in *p*-dioxane, this work)

[f] PCM (B3LYP/A in *p*-dioxane, this work)

[g] PCM (MP2/A in *p*-dioxane, this work)

According to results of Table 2, it can be seen that the α_{yy} component is the highest contribution to the linear polarizability of these compounds. However, there is a small difference between this component and the α_{xx} one. In terms of the employed methods, the HF approach gives the lowest polarizability values. The extension of the basis sets increase the α property, until a relative saturation, giving positive effects to the polarizability tensor. Following the effects of electron correlation we can see that all the employed correlated methods increase the α properties of these isomers with respect to the HF ones. In particular, from the supplementary material, we can see that the B3LYP method with different basis sets project the highest values of α_{ave}. In particular, the performance of the HF and B3LYP methods with the large 6-311+G(3d,3p) basis set gives α_{ave} results that increase approximately by 5% with respect to the values calculated with the 6-31+G(d,p). For the ONP and PNP isomers, the B3LYP/6-311++G(3d,3p) calculated α_{ave} is able to reproduce approximately the 95% of their static experimental values. For MNP isomer, the value of α_{ave} slightly overestimates the experimental value by 8%. Furthermore, B3LYP/B methodology is able to give α values that are comparable to those calculated by using the CAM-B3LYP/Sadlej and MP2/Sadlej ones. In relation to the MP2 calculations, the corresponding α_{ave} values for ONP and PNP reproduce the 90% of the experimental ones.

For MNP, the MP2 α_{ave} value is coincident to the experimental one. However, the slight differences between the theoretical values (gas phase) and experimental ones [13], can be mainly attributed to solvent effects. It is worth to mention that the present α_{ave} calculations are more consistent to the experimental ones than the results by Bursi et al. [16] using the SOO methodology at HF/TZVP level, which differs in 20% with respect to the experimental measurements, the values of which are smaller than the theoretical ones. Furthermore, our gas phase results follow exactly the experimental tendency of the measured dipole polarizability of nitrophenol compounds in solution.

With respect to the MP4 electron correlation effects, it is observed that this order of perturbation corrects the positive contributions to the α_{ii} components as it is observed for MP2 and DFT results, indicating that the real solvent effects could induce significant variations in the gas phase polarizabilities of nitrophenol compounds. This result is confirmed by CCSD/A calculations, that give polarizability component values that are still lower than MP4 (see Table 2 for PNP isomer). In fact, B3LYP/A and MP2/A calculations for the PNP isomer using *p*-dioxane as solvent with the Onsager (α_{ave} (B3LYP/A) = 120.18 au) and SCRF-PCM (α_{ave} (B3LYP/A) = 124.07 au, α_{ave} (MP2/A) = 120.28 au) models, which results are also included in Table 2, indicate that the solvent effects are able to reproduce reasonably the experimental dipole polarizabilities of the studied isomers. Similar behavior is observed for the PNA calculations, where the MP4/Sadlej method give a value of α_{ave} = 103.73 au that is comparable to the CCSD/aug-cc-pvTZ one (α_{ave} = 104.25 au, Ref. [7]), where both of these values are smaller than the corresponding values measured in acetone (α_{ave} = 114.73 au). Further investigation about the subject of the impact of the existent methodology for evaluating the dipole polarizabilities of molecules in solution is under way in our laboratory.

3.3 First hyperpolarizability (β)

Table 3 shows the values of β_v and the longitudinal (β_{yyy}) and cross (β_{yxx}, β_{yzz}) components for the nitrophenol isomers, where the β_{yyy} components represent the highest contribution to the β_v property of these compounds according to orientation of Fig. 1. This component lies into the dipole moment direction, determined by the orientation of the nitro group located along the *y*-axis of the molecular system. As for the dipole moment and the dipole polarizability results, the HF and B3LYP β calculations are displayed as supplementary material.

The B3LYP, CAMB3LYP and MP2 results show that the electron correlation effects at these levels of theory increase significantly the β_v property with respect to the calculated HF values. For instance, the B3LYP β_v values for the ONP compound are 4 times higher than the HF, whereas this relationship is approximately 6 times for the MP2. For the case of MNP and PNP, the β_v property increase three and two times, respectively, with both

Table 3 Calculated β_{yyy}, β_{yxx}, β_{yzz} components and β_v static first hyperpolarizability (au) values of ONP, MNP and PNP isomers

Molecule	β_v (au)	CAM-B3LYP			MP2			MP4			CCSD
		A	B	C	A	B	C	A	B	C	A
ONP	β_{yyy}	529.6	505.4	491.2	650.1	616.4	615.8	466.9	449.1	452.2	
	β_{yxx}	−8.4	−6.8	−3.3	−48.7	−47.0	−47.2	−90.5	−90.1	−89.5	
	β_{yzz}	−91.8	−72.9	−64.9	−79.8	−71.2	−65.8	−69.6	−60.4	−55.0	
	β_v	143.1	141.8	140.9	173.9	166.1	167.6	102.3	99.6	102.6	
MNP	β_{yyy}	491.4	446.5	479.5	468.6	473.5	490.1	304.6	307.8	326.3	
	β_{yxx}	−197.1	−175.9	−185.3	103.4	75.8	71.7	65.0	39.5	36.5	
	β_{yzz}	−15.3	−16.1	−9.3	−40.3	−36.6	−29.8	−32.6	−30.1	−23.6	
	β_v	93.0	84.8	94.9	177.2	170.9	177.3	112.4	105.8	113.1	
PNP	β_{yyy}	1,141.5	1,068.8	1,077.1	1,152.2	1,089.6	1,107.6	927.1	869.8	892.3	1,006.8
	β_{yxx}	−84.8	−79.7	−81.2	−34.0	−33.8	−32.1	−74.8	−73.6	−71.8	−82.4
	β_{yzz}	−24.2	−22.9	−15.9	−23.1	−21.8	−13.3	−17.6	−16.9	−8.6	−17.8
	β_v	344.2	322.1	326.6	365.1	344.6	354.1	278.2	259.8	270.6	302.2
PNA	β_{yyy}	2,194.2	2,033.2	2,094.5	2,184.8	2,017.7	1,996.8	1,804.2	1,646.6	1,633.9	1,759.3[a]
	β_{yxx}	−59.3	−55.7	−59.4	−64.4	−63.8	−63.2	−106.9	−105.4	−104.2	−117.7[a]
	β_{yzz}	−257.4	−236.9	−235.7	−65.4	−62.2	−63.9	−54.4	−51.4	−52.7	−54.5[a]
	β_v	625.8	580.2	599.8	685.0	630.6	623.2	547.6	496.6	492.4	529.0[a]

Values for PNA are included for comparison. The basis sets are: *A* = 6-31+G(d.p), *B* = 6-311++G(3d.3p) and *C* = Sadlej

[a] CCSD/aug-cc-pVTZ. Ref. [7]

methods. These results confirm the very well-known fact about the importance of including electron correlation in the calculation of nonlinear optical properties. With respect to the differences due to the employed atomic functions, the β results show that there are no large basis set effects in the present calculations. For the studied isomers, the tendency for the β_v values of Table 3 is the following: β_v PNP $>$ β_v MNP $>$ β_v ONP. The inclusion of higher order correlation effects in β calculations, such as MP4-SDQT (shown in Table 3), tend to correct the MP2 positive contributions (higher than DFT ones in some cases) and stabilizing the first hyperpolarizability along the series of the A, B and C basis sets. For instance, for the ONP, MNP and PNP isomers, the MP4 β_v values are saturated around 102 au, 112 au and 278 au, respectively. For the case of PNP isomer, the β_v (MP4) value is comparable to the corresponding CCSD/A present calculations ($\sim$300 au), displayed in Table 3.

Table 3 also report results for PNA molecules at these levels of theory. In particular, it is important to mention that the MP4 β_v property goes from 547.6 (MP4/6-31+G(d,p) to 492.4 (MP4/Sadlej) and these results are very close to that recently reported for PNA at the CCSD/aug-cc-pvTZ (529.0 au) level of theory [7].

In Table 4, the static β_v values in gas phase for the studied isomers in esu units are presented. Additionally, we present the calculated MP2/A dynamic β_v values at 1,910 nm to be compared with the dynamic experimental ones [13] (ω = 1,910 nm, using dioxane as solvent) and other dynamic values from the literature [16, 17]. The corresponding HF/A and B3LYP/A results are reported as supplementary material.

A comparison between our theoretical results (determined by using B conversion factor [47]) and the experimental hyperpolarizability results is expected [13]. However, a direct differentiation between experiment–theory of the NLO properties is many times difficult [47, 48], because in real nonlinear optical experiments the observed NLO property P_t can be represented as the overall consequence of different contributions, such as: (a) static (electronic (P_0^e) and nuclear (P_0^n)), (b) dependence of frequency of the applied electric field ($P_v^e + P_v^e$), (c) orientation of molecules, and d) solvent effects, among others. From these contributions, the experience has demonstrated that the static electronic contribution P_0^e, referred as the intrinsic nonlinear optical response of the electronic charge density, is the determinant part to the macroscopic nonlinear optical property. In fact, our present results only correspond to the electronic contribution of the optical properties.

For the dynamic contribution, the β_v results at 1,910 nm are increased by 5% with respect to the static β_v values, whereas the B3LYP and MP2 dynamic values reproduce the experimental values of ONP in 40 and 66%, respectively. For the PNP isomer, the corresponding results represent approximately the 60% of the experimental, and for the MNP the calculated values by both methods are comparable with the experimental value of β.

Likewise, the present results for the PNP isomer are consistent with the values reported by Bursi et al. [16], unlike to those reported by Guthmuller and Simon [17], where the corresponding static and dynamic properties are overestimated.

For the studied nitrophenols, the tendency for the present β_v calculations is the following: β_v PNP $>$ β_v MNP $>$ β_v ONP, which is not coincident to that reported by Bursi et al. [16] and that experimental one (β_v PNP $>$ β_v ONP $>$ β_v MNP) due to Cheng et al. [13]. However, Cheng et al. [13] have also reported at experimental level the NLO properties of nitrobenzene derivatives, finding that the formation of an intramolecular hydrogen bond in the *ortho*-isomers may decrease in some cases the expected β responses, where for these isomers the tendency for the first hyperpolarizability is β *para* $>$ β *meta* $>$ β *ortho*, which coincides exactly with the values reported in the present work.

Due to the difference between the experimental and theoretical tendency in the β results, solvent effect calculations were performed for the first hyperpolarizability of these molecules in presence of *p*-dioxane at static level, using the Onsager and SCRF-PCM models and the B3LYP/A and MP2/A methods. The corresponding results, also shown in Table 4, indicate that at the B3LYP level there are no significant differences between the Onsager and PCM β solvent effect calculations. However, the β properties obtained with the DFT-PCM model are consistent with the MP2-PCM calculations. With respect to the trend

Table 4 Theoretical (static and dynamic) and experimental (dynamic) first hyperpolarizability β_v values (10^{-30} esu) for the ONP, MNP and PNP isomers

Molecule	ω (nm)	MP2/A	MP2/A(PCM)	Other studies	Exp[c]
ONP	0	0.751	0.936 (0.57)	0.812[a]	–
	1,910	0.786		–	1.2
MNP	0	0.766	1.413 (0.90)	0.565[a]	–
	1,910	0.802		–	0.8
PNP	0	1.577	4.023 (3.07)	1.534[a]; 4.83[b]	–
	1,910	1.648		5.78[b]	3.0
PNA			6.095 (4.82)		8.1[d]

Additional MP2/A(PCM) β_v (10^{-30} esu) values for ONP, MNP, PNP and PNA molecules in *p*-dioxane The basis set is A = 6-31+G(d,p)

[a] Theoretical values by SOO-HF/DZ; Ref. [16]

[b] Theoretical values by DFT: SAOP/TZ2P; Ref. [17]

[c] Experimental EFISH measurements in *p*-dioxane; Ref. [13]

[d] Experimental (EFISH at zero frequency in *p*-dioxane); Ref. [14]

of these values, results of Table 4 show that solvent effects results follow exactly the static and dynamic β calculated tendency in absence of solvent. In particular, we can observe that the B3LYP/6-31+G(d,p) $\beta(10^{-30}$ esu) follow the pattern: $\beta_{v(\text{diox})}$ ONP = 0.829; $\beta_{v(\text{diox})}$ MNP = 1.380; $\beta_{v(\text{diox})}$ PNP = 2.774, which is similar to previous values. However, β results in presence of the solvent are increased by almost 70% with respect to the gas phase values at the same level of theory. These results reveal the importance of solvent effects on the NLO properties and which is currently the subject of investigation in our laboratory, not only at static level but including the dynamic effects. Additionally, Table 4 shows (in parentheses) the MP2(PCM) β values corrected by the MP4/MP2 corresponding results from Table 3, which indicate that MP2 with solvent effects also overestimate the first hyperpolarizability as shown for the static hyperpolarizabilities. However, static corrections with higher order electron correlation methods, such as MP4 ones, can give β values that can describe the right experimental measurements.

An analysis of the natural population (NPA) and the Mulliken atomic population (MAP) on the oxygen atoms of the $-NO_2$ group of the nitrophenol isomers (see Table 5) can explain the tendency of the first hyperpolarizability observed in this work. The delocalization of electronic density of the nitro group is given by the resonance structures (1) and (2) and an average of these two structures can be represented through the structure (3) as shown in Fig. 2. The variation of the charge of O_x oxygen with respect to O_y oxygen using the B3LYP method (displayed in Table 1.4 of supplementary material) shows the following differences 13, 22 and 89% for the PNP, MNP and ONP, respectively. These variations also hold with the rest of methods employed in this work. The biggest charge difference observed for ONP isomer can be attributed to the formation of the intramolecular hydrogen bond between the O_y and H_y atoms that reduce the degree of electronic density delocalization in between the $-NO_2$ group and the aromatic ring, with the reduction in the hyperpolarizability response. To have accurate description of these changes, MAP and NPA charges were calculated

Table 5 Calculated Mulliken Atomic Charge (q) and natural population analysis (NPA) for the O_x and O_y oxygen atoms of the ONP, MNP and PNP, at the level MP2/6-31+G(d,p)on MP2 optimized geometries

Molecule	qO_x	qO_y	NPA O_x	NPA O_y
ONF	−0.161	−0.281	−0.323	−0.392
MNF	−0.182	−0.198	−0.337	−0.346
PNF	−0.205	−0.207	−0.349	−0.348
PNA	−0.215	−0.215	−0.361	−0.361

Values for PNA are included as reference

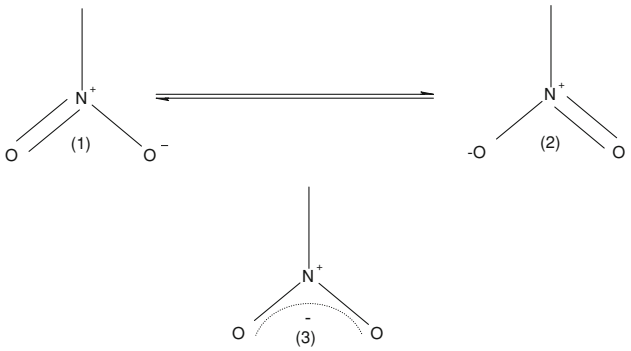

Fig. 2 Resonance structures for the $-NO_2$ group

at MP2/6-31+G(d,p) level using optimized geometries at the same level. The following order of these charges is PNP > MNP > ONP, that coincides with the tendency for our β results. Figure 3 shows that there exists an exponential relationship ($r^2 = 0.98$) between the β_v and the O_x atomic change (NPA) for the isomers at [MP2/6-31+G(d, p)] level of theory. Likewise, we have determined the qO_x and the NLO properties for PNA. These properties were included in Fig. 3 with the aim of showing this behavior clearly. MAP and NPA charges give coincident behavior for nitrophenol isomers, including the PNA as reference.

3.4 Second hyperpolarizability (γ)

Table 6 displays the values of the components that contribute to the second hyperpolarizability tensor and the γ_{ave} scalar of the ONP, MNP and PNP isomers. The HF and B3LYP are included as supplementary material. Similar to α_{yy} and β_{yyy}, the higher order component is the γ_{yyyy}.

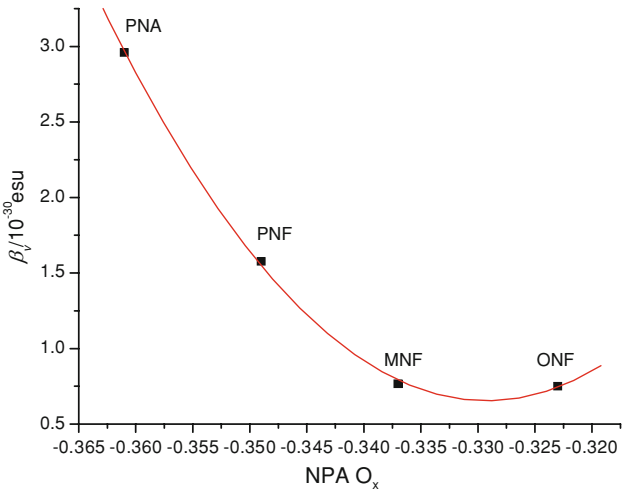

Fig. 3 Relationship between the first hyperpolarizability β_v and the NPA O_x charge of the oxygen atom of the ONP, MNP, PNP and PNA molecules, calculated with the MP2/6-31+G(d,p) methodology

Table 6 Calculated static values of the components and the average of the second hyperpolarizability of ONP, MNP and PNP isomers

Molecule	γ_{ave} (au)	CAM-B3LYP			MP2			MP4			CCSD/A
		A	B	C	A	B	C	A	B	C	
ONP	γ_{xxxx}	10,638	11,074	13,793	7,980	8,641	11,939	8,634	9,194	12,250	
	γ_{yyyy}	29,584	28,955	33,072	52,970	50,132	54,425	44,665	42,447	46,581	
	γ_{zzzz}	9,814	7,737	9,629	10,491	8,650	10,746	9,949	7,920	9,950	
	γ_{xxyy}	6,067	6,076	7,159	3,034	3,331	4,552	4,046	4,003	5,175	
	γ_{xxzz}	4,421	3,983	5,069	4,944	4,709	5,801	4,606	4,283	5,272	
	γ_{yyzz}	3,990	3,856	4,967	3,985	4,006	5,297	3,770	3,634	4,985	
	γ_{ave}	1,5799	15,120	18,177	19,073	18,303	21,682	17,619	16,680	19,929	
MNP	γ_{xxxx}	1,1416	1,2445	13,836	10,954	10,707	13,116	11,696	11,231	13,659	
	γ_{yyyy}	29,648	30,566	31,387	52,141	49,122	52,444	39,754	37,666	40,895	
	γ_{zzzz}	10,675	7,357	8,997	10,695	8,114	9,915	9,974	7,383	8,986	
	γ_{xxyy}	11,415	10,957	11,480	1,280	1,672	2,614	2,581	2,665	3,554	
	γ_{xxzz}	5,264	4,090	4,861	5,069	4,459	5,318	4,689	4,017	4,759	
	γ_{yyzz}	3,458	2,865	3,718	3,403	3,072	4,090	3,258	2,891	3,776	
	γ_{ave}	18,402	17,238	18,868	18,659	17,270	19,904	16,496	15,085	17,544	
PNP	γ_{xxxx}	1,0551	7,303	12,310	7,493	7,822	10,026	8,692	8,544	10,516	6,836
	γ_{yyyy}	5,377	52,281	56,782	89,320	83,683	87,491	73,262	68,310	72,651	75,068
	γ_{zzzz}	9,649	9,571	9,016	10,624	8,072	9,484	9,959	7,360	8,896	9,634
	γ_{xxyy}	9,852	9,298	10,480	−812	−117	631	516	1,006	1,733	−830
	γ_{xxzz}	4,922	3,820	4,699	5,199	4,707	5,401	4,768	4,194	4,750	4,603
	γ_{yyzz}	2,895	2,465	3,541	2,392	2,233	3,026	2,394	2,195	3,190	2,156
	γ_{ave}	22,383	20,064	23,110	24,199	22,645	25,024	21,454	19,801	22,282	20,679
PNA	γ_{xxxx}	11,364	8,544	10,807	8,435	8,729	11,082	9,634	9,411	11,826	
	γ_{yyyy}	96,010	89,904	102,024	168,522	156,204	164,124	139,292	127,914	135,662	
	γ_{zzzz}	11,704	10,884	13,147	12,176	9,850	12,385	11,428	8,899	10,879	
	γ_{xxyy}	213	859	1,505	−3,771	−2,365	−1,433	−2,122	−1,016	132	
	γ_{xxzz}	5,768	4,441	6,232	5,674	5,339	6,379	5,158	4,666	5,643	
	γ_{yyzz}	3,940	3,964	5,470	3,887	4,171	6,562	3,812	3,838	5,970	
	γ_{ave}	27,784	25,572	30,479	40,143	37,815	42,122	34,810	32,240	36,371	

Values for PNA are included for comparison. The basis sets are A = 6-31+G(d,p), B = 6-311++G(3d,3p) and C = Sadlej

The calculated γ_{ave} with the 6-311++G(3d,3p) basis set tend to decrease with respect to the 6-31+G(d,p) values. However, these differences are smaller than 10%. The values of γ_{ave} obtained with the HF/6-31+G(d,p) methodology are underestimated by around 40% in relation to the B3LYP/6-31+G(d,p) and MP2 results. Once again, we can confirm the importance of electron correlation in the calculation of third order NLO properties. The main features of these results are that B3LYP and CAMB3LYP methods are able to give comparable γ_{ave} values when they use the same basis sets. For the case of CAM-B3LYP/Sadlej, it is observed that the γ_{ave} increases for all the cases. With respect to the inclusion of higher order correlation effects at MP2, the values of γ_{ave} increases with respect to those calculated at DFT level but remain almost constant along the A, B and C series of basis sets. When the MP4 correlation is considered, the positive contributions observed in MP2 calculations are corrected, which continue to be corrected at the CCSD/A level of theory. It is important to note that the tendency for γ_{ave} with the ab initio method (γ_{ave} ONP > γ_{ave} MNP < γ_{ave} PNP) is different to that determined by the DFT ones (γ_{ave} ONP < γ_{ave} MNP < γ_{ave} PNP). Likewise, the tendencies for the γ_{yyyy} components follow the same behavior corresponding to the γ_{ave} ab initio and DFT methods. Further research in this field is being carried out in our laboratory, in order to clarify these tendencies.

Table 7 shows the dynamic and static γ_{ave} values in esu units calculated with different methods, and the reported values from the literature [11, 13–16]. The dynamic γ_{ave} values are increased by 10% with respect to the static ones. The tendency for the B3LYP γ_{ave} values follows the same behavior reported by Cheng et al. [13] from experimental results. Figure 4 shows an exponential relationship

Table 7 Theoretical and experimental second hyperpolarizability values (10^{-36} esu) for the ONP, MNP and PNP isomers

Molecule	ω (nm)	HF	B3LYP	MP2	MP4	Other theoretical studies	Exp
ONP	0	1.003	1.367	1.601	1.479	0.972[a]	–
	1,910	1.111	1.514	1.773	1.638		3[b]
MNP	0	0.971	1.728	1.566	1.385	0.946[a]	–
	1,910	1.064	1.894	1.716	1.518		6[b]
PNP	0	1.107	2.000	2.031	1.801	1.155[a]	–
	1,910	1.233	2.228	2.262	2.006	–	8[b]
PNA	0	1.606	2.351	3.370	2.922	3.24[e]	6.9[d]
	1,910	1.863	2.691	3.632	2.904	–	15[c]

Values for PNA are included for comparison. A = 6-31+G(d, p)

[a] Theoretical values at SOO-HF/TZV level; Ref. [16]

[b] Experimental THG measurement in *p*-dioxane at 1,910 nm; Ref. [13]

[c] Experimental THG measurement in acetone at 1,910 nm; Ref. [13]

[d] Femtosecond Z-scan measurements in DMSO at zero frequency; Ref. [15]

[e] B3LYP/6-31+G(d*,p), Ref. [11]

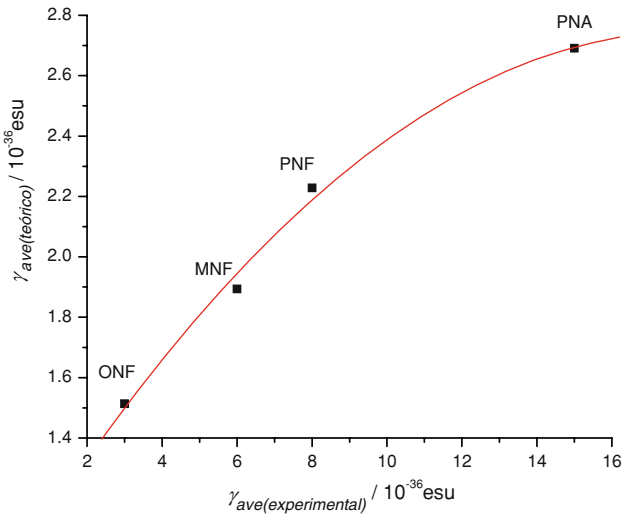

Fig. 4 Relationship between the calculated γ_{ave} B3LYP/6-31+G(d,p) and the experimental γ_{ave} (THG measured at 1,910 nm) of the ONP, MNP, PNP and PNA molecules. Correlation coefficient $r^2 = 0.99$

($r^2 = 0.99$) between the theoretical and experimental γ_{ave} (at 1,910 nm) property. Additionally, we have included the theoretical and experimental γ_{ave} of the PNA at 1,910 nm. The calculated γ_{ave} at 1,910 nm with the DFT method represent approximately the 50, 32 and 28% the values of the experimental γ_{ave} for ONP, MNP and PNP, respectively. The behavior of the B3LYP γ_{ave} values in terms of the qO_x atomic charge is similar to the relationship for β_v results (see Fig. 5). The tendencies with the HF, MP2 and MP4 results are coincident to those reported by Bursi et al. [16].

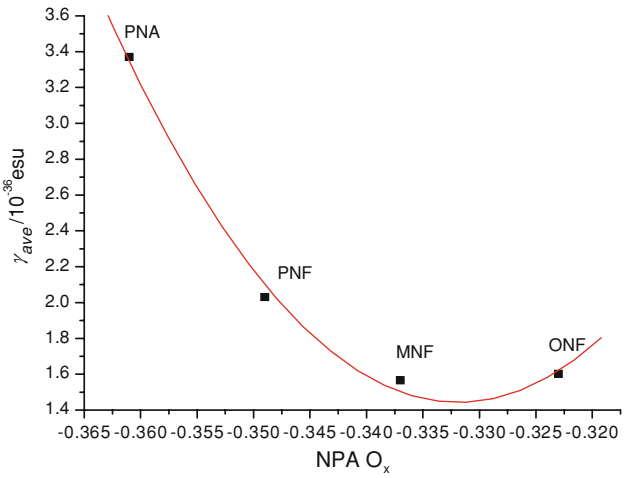

Fig. 5 Relationship between the second hyperpolarizability γ_{ave} and the NPA O_x charge of the oxygen atom of the ONP, MNP, PNP and PNA molecules, calculated with the MP2/6-31+G(d,p) methodology

Finally, despite the β and γ theory–experiment differences that lie between 40% and 70%, it is important to emphasize that the present study has considered only the electronic and dynamic contribution to the NLO properties of nitrophenol isomers in gas phase. For the case of β, solvent effect calculations were performed additionally. However, for a better direct theory–experiment comparison it is necessary to evaluate other factors (as mentioned previously) that can provide the contribution to the total molecular optical property. These factors were not considered in this study. However, we are addressing research in this direction.

4 Conclusions

The MP2 and B3LYP methods with the 6-31+G(d,p) and 6-31++G(3d,3p) basis sets allow to obtain results of α_{ave}, β_v and γ_{ave} that can be considered acceptable for comparing with the corresponding experimental values of the *ortho*-, *meta*- and *para*-nitrophenol isomers (ONP, MNP and PNP). CAMB3LYP and MP4 methods, with specialized basis sets, such as Sadlej one, must be employed to achieve a good correspondence theory–experiment. The tendency for the calculated β_v property (β_v PNP > β_v MNP > β_v ONP) differs to the experimental one (β_v PNP > β_v ONP > β_v MNP). However, this difference has been explained in terms of the variations of O_x atomic charge of the $-NO_2$ group ($r^2 = 0.98$) as results of one intramolecular OH bonding that reduce the first hyperpolarizability. In the case of γ_{ave}, there exist significant differences of until 72% in comparison to the experimental results. However, the tendency with the B3LYP results is in correspondence to the experimental reports ($r^2 = 0.99$).

Finally, the use of finite field methodology in combination with the B3LYP, CAMB3LYP, MP2 and MP4 methods using the 6-31+G(d,p), 6-311++G(3d,3p) and Sadlej basis can be combined as an appropriate alternative to predict the optical properties of Push–Pull type organic molecules. MP4/Sadlej approach is able to give nonlinear optical properties that are in good correspondence with more sophisticated CCSD calculations.

Acknowledgment This work was totally supported by the project of CONDES No.: CC-0913-07 of La Universidad del Zulia.

References

1. Delaire JA, Naakatani K (2000) Chem Rev 100:1817–1845
2. Bredas JL, Adant C, Tackx P, Persoons A, Pierce BM (1994) Chem Rev 94:243–278
3. Arivuoli D (2001) Pramana J Phys 57:871–883
4. Corn RM, Higgins DA (1994) Chem Rev 94:107–125
5. Shelton DP, Rice JE (1994) Chem Rev 94:3–29
6. Kanis DR, Ratner MA, Marks TJ (1994) Chem Rev 94:195–242
7. Hammond JR, Kowalski K (2009) J Chem Phys 130:194108
8. Cole J (2003) Phil Trans R Soc Lond 361:2751–2770
9. Champagne B (1996) Chem Phys Lett 261:57–65
10. Sim F, Steven C, Dupuis M, Rice J (1993) J Phys Chem 97:1158–1163
11. Soscún H, Castellano O, Bermúdez Y, Toro C, Cubillán N, Hinchliffe A, Nguyen-Phu X (2006) Int J Quantum Chem 106:1130–1137
12. Moran AM, Kelley AM (2001) J Chem Phys 115:912–924
13. Cheng LT, Tam W, Stevenson SH, Meredith GR, Rikken G, Marder SR (1991) J Phys Chem 95:10631–10643
14. Stahelin M, Burland DM, Rice JE (1992) Chem Phys Lett 191:245–250
15. Audebert P, Kamada K, Matsunaga K, Ohta K (2003) Chem Phys Lett 367:67–71
16. Bursi R, Lankhorst M, Feil D (1995) J Comp Chem 16:545–562
17. Guthmuller J, Simon D (2006) J Chem Phys 124:174502
18. MP2: Gordon MH, Pople JA, Frisch MJ (1988) Chem Phys Lett 153:503–506
19. MP4: Krishnan R, Pople JA (1978) Int J Quantum Chem 14:91–100
20. Trucks GW, Watts JD, Salter EA, Bartlett RJ (1988) Chem Phys Lett 153:490–495
21. Becke AD (1988) Phys Rev A 38:3098
22. Yang LW, Parr RG (1988) Phys Rev B 37:785
23. Becke AD (1993) J Chem Phys 98:5648–5662
24. Yanai T, Tew DP, Handy NC (2004) Chem Phys Lett 393:51–57
25. Frisco MJ, Pople, JA, Binkley JS (1984) J Chem Phys 80:3265–3269
26. Sadlej A (1988) Collect Czech Chem Commun 53:1995–2016
27. Sadlej AJ, Urban M (1991) Theochem 234:147–171
28. Sadlej A (1991) Theo Chim Acta 79:123–140
29. Cernusak I, Kello V, Sadlej J (2003) Collect Czech Chem Commun 68:211–239
30. Monkhorst JR (1977)Int J Quantum Chem S11:421–432
31. Cohen HD, Roothaan CCJ (1965) J Chem Phys 43:S34–S39
32. Kurtz HA, Stewart JP, Dieter KM (1990) J Comp Chem 11:82–87
33. Gaussian: Frisch MJ, Trucks GW, Schlegel HB, Scuseria GE, Robb MA, Cheeseman JR, Montgomery JA Jr, Vreven T, Kudin KN, Burant JC, Millam JM, Iyengar SS, Tomasi J, Barone V, Mennucci B, Cossi M, Scalmani G, Rega N, Petersson GA, Nakatsuji H, Hada M, Ehara M, Toyota K, Fukuda R, Hasegawa J, Ishida M, Nakajima T, Honda Y, Kitao O, Nakai H, Klene M, Li X, Knox JE, Hratchian HP, Cross JB, Adamo C, Jaramillo J, Gomperts R, Stratmann RE, Yazyev O, Austin AJ, Cammi R, Pomelli C, Ochterski JW, Ayala PY, Morokuma K, Voth GA, Salvador P, Dannenberg JJ, Zakrzewski VG, Dapprich S, Daniels AD, Strain MC, Farkas O, Malick DK, Rabuck AD, Raghavachari K, Foresman JB, Ortiz JV, Cui Q, Baboul AG, Clifford S, Cioslowski J, Stefanov BB, Liu G, Liashenko A, Piskorz P, Komaromi I, Martin RL, Fox DJ, Keith T, Al-Laham MA, Peng CY, Nanayakkara A, Challacombe M, Gill PMW, Johnson B, Chen W, Wong MW, Gonzalez C, Pople JA (2003) Gaussian, Inc., Pittsburgh, PA
34. Dallton 2.0 (2005) Supplemented with the CAMB3LYP patch: DALTON, a molecular electronic structure program, Release 2.0. http://www.kjemi.uio.no/software/dalton/dalton.html
35. Schmidt M, Baldridge K, Boatz J, Elbert S, Gordon M, Jensen J, Koseki S, Matsunaga N, Nguyen K, Su S, Windus T, Dupuis M, Montogomery J (2002) Gamess version, February 2002
36. Schmidt M, Baldridge K, Boatz J, Elbert ST, Gordon MS, Jensen JH, Koseki S, Matsunaga N, Nguyen KA, Su SJ, Windus TL, Dupuis M, Montgomery JA (1993) J Comp Chem 14:1347–1363
37. Kanis DR, Ratner MA, Marks TJ (1994) Chem Rev 94:195–242
38. Wong MW, Frisch MJ, Wiberg KB (1991) J Am Chem Soc 113:4776–4782
39. Onsager L (1936) Am Chem Soc 58:1486
40. Cammi R, Mennucci B, Tomasi J (2000) J Phys Chem A 104:5631–5637
41. Cossi M, Scalmani G, Rega N, Barone V (2002) J Chem Phys 117:43–54
42. Iwasaki F, Kawano Y (1978) Acta Crystallogr B 34:1286–1290
43. Hamzaoui F, Baert F, Wojcik G (1996) Acta Crystallogr B 52:159–164
44. Pandarese F, Ungaretti L, Coda A (1975) Acta Crystallogr B 31:2671–2675
45. Coppens P, Schmidt GMJ (1965) Acta Crystallogr 18:654–663
46. Coppens P, Schmidt GMJ (1965) Acta Crystallogr 18:62–67
47. Willetts A, Rice JE, Burland DM (1997) J Chem Phys 97:7590–7599
48. Reis H (2006) J Chem Phys 125:014506–014511